



This is a repository copy of *Investigating a novel Ag/ZnO based hybrid nanofluid for sustainable machining of inconel 718 under nanofluid based minimum quantity lubrication.*

White Rose Research Online URL for this paper:
<https://eprints.whiterose.ac.uk/173569/>

Version: Accepted Version

Article:

Barewar, S.D., Kotwani, A., Chougule, S.S. et al. (1 more author) (2021) Investigating a novel Ag/ZnO based hybrid nanofluid for sustainable machining of inconel 718 under nanofluid based minimum quantity lubrication. *Journal of Manufacturing Processes*, 66. pp. 313-324. ISSN 1526-6125

<https://doi.org/10.1016/j.jmapro.2021.04.017>

© 2021 The Society of Manufacturing Engineers. This is an author produced version of a paper subsequently published in *Journal of Manufacturing Processes*. Uploaded in accordance with the publisher's self-archiving policy. Article available under the terms of the CC-BY-NC-ND licence (<https://creativecommons.org/licenses/by-nc-nd/4.0/>).

Reuse

This article is distributed under the terms of the Creative Commons Attribution-NonCommercial-NoDerivs (CC BY-NC-ND) licence. This licence only allows you to download this work and share it with others as long as you credit the authors, but you can't change the article in any way or use it commercially. More information and the full terms of the licence here: <https://creativecommons.org/licenses/>

Takedown

If you consider content in White Rose Research Online to be in breach of UK law, please notify us by emailing eprints@whiterose.ac.uk including the URL of the record and the reason for the withdrawal request.



eprints@whiterose.ac.uk
<https://eprints.whiterose.ac.uk/>

1 **Investigating a novel Ag/ZnO based hybrid nanofluid for sustainable**
2 **machining of Inconel 718 under nanofluid based minimum quantity**
3 **lubrication**

4 Surendra D. Barewar¹, Aman Kotwani¹, Sandesh S. Chougule¹, Deepak Rajendra Unune^{1,2*}

5 ¹Department of Mechanical-Mechatronics Engineering, The LNM Institute of Information
6 Technology, Jaipur-302031, Rajasthan, India

7 ²Department of Materials Science and Engineering, INSIGNEO Institute of *in silico*
8 Medicine, University of Sheffield, Sheffield - S1 3BJ, United Kingdom.

9 *Corresponding Author

10 Email: d.unune@sheffield.ac.uk; Contact: +44 7424011698

11
12 **Abstract**

13 Sustainable machining, with implementation of eco-friendly dry and minimum quantity
14 lubrication (MQL) methods, has gained attraction of researchers and engineers to solve the
15 environmental and health allied issues caused by bulk usage of the conventional cutting fluids.
16 Nanofluids have recently become more obvious choice as a cutting fluid in MQL applications
17 owing to their superior thermo-physical properties. In this work, a novel hybrid nanofluid,
18 consisting of Ag coated ZnO (Ag/ZnO) nanoparticles in ethylene glycol base, has been
19 proposed as cutting fluid for MQL application. Initially, the Ag/ZnO hybrid nanoparticles were
20 synthesized by a chemical precursor method. Then, synthesized nanoparticles were blended in
21 ethylene glycol at several volume concentrations ($\Phi = 0.05\%$ to 0.2%). The nanofluids were
22 characterized for their thermo-physical properties and stability criterion, and then a nanofluid
23 with the best performance was selected for nanofluid based MQL (NFMQL) experiments. The
24 performance of NFMQL was compared with dry, MQL environments during milling of
25 difficult-to-cut Inconel 718 superalloy with PVD coated carbide inserts. Taguchi L9 orthogonal
26 array was incorporated for experimental design to investigate the effect of cutting speed, feed

27 rate and machining environment on the machining performance in terms of the average surface
28 roughness and cutting temperature. Analysis of variance shown that the cutting environment
29 contributed to the average surface roughness and cutting temperature by 24.52 % and 44.74%,
30 respectively. As compared to dry and MQL condition, the NFMQL improved the surface finish
31 by 23.5 % and 13.07 %, respectively, and reduced the cutting temperature by 15.38 % and 8.56
32 %, respectively, owing to proposed hybrid nanofluids enhanced lubrication and heat dissipation
33 properties. Furthermore, the field emission scanning electron microscopic (FESEM) images of
34 used cutting tool inserts reveal that the NFMQL condition induces the minimum tool wear as
35 compared with MQL and dry environments. Finally, the multi-response optimization was
36 achieved through the implementation of Taguchi grey relational analysis (TGRA) with the
37 optimum combination of cutting speed of 30 m/min, feed rate of 0.036 mm/tooth, and NFMQL
38 cutting environment.

39 **Keywords:** Sustainable machining, MQL, NFMQL, Milling, Inconel 718, Hybrid nanofluid.

40 **Nomenclature:**

41 MQL: minimum quantity lubrication

42 NFMQL: nanofluid based minimum quantity lubrication

43 CNC: computer numerical control

44 CBN: cubic boron nitride

45 MRR: material removal rate

46 MWCNT: multi-walled carbon nanotube

47 SDS: sodium dodecyl sulfate

48 PVA: poly vinyl alcohol

49 FESEM: field emission scanning electron microscope

50 EDX: energy dispersive x-ray

- 51 BUE: built-up-edge
52 DOF: degree of freedom
53 R_a : average surface roughness
54 μ : viscosity
55 Φ : volume concentration
56 ρ : density
57 *hn*: hybrid nanofluid
58 *bf*: base fluid
59 ANOVA: Analysis of variance
60 S/N ratio: Signal-to-noise ratio
61 TGRA: Taguchi grey relational analysis
62 GRG: grey relational grade

63 **1. Introduction**

64 Conventional machining of difficult-to-cut Inconel 718 has always been challenging operation
65 owing to severe cutting tool wear, deprived surface finish, problems in chip formation, and,
66 more importantly, poor dissipation of excessive heat generated at cutting zone. Due to the
67 promising properties viz. high-temperature strength, best corrosion and fatigue resistance,
68 Inconel 718 superalloy finds numerous applications in atomic reactor, aviation parts, food
69 processing and chemical equipment and heavy-duty marine machinery [1]. However, those
70 superior properties also make Inconel 718 a difficult-to-cut material. To ease the machining,
71 the practice of metal working fluids (MWF's) in flood lubrication mode is a typical strategy
72 adopted in industries for dissipation of heat liberated in the machining of such difficult-to-cut
73 materials. The flood lubrication generally improves the machining performance by dissipating
74 the heat released at the cutting region and yields a better surface finish, tool life and chip
75 removal [2]. However, the bulk uses of the MWF's in flood lubrication often account for 16-

76 20% of total machining costs, in addition to their handling and management costs. MWF's
77 result in health hazards and leads to environmental pollution [2]. Furthermore, the MWF's tend
78 to degrade with time due to bacterial growth and also requires treatment before dumping into
79 the sewage system [3].

80 Global responsiveness towards sustainable manufacturing and customer's awareness about the
81 environment friendly products has derived the attention of machining industries to abate or
82 abolish the use of MWF's. In this regard, several alternatives like cryogenic lubrication, dry
83 machining, minimum quantity lubrication (MQL) and solid lubricant assisted machining have
84 been investigated and developed. Among these alternatives, researchers, of late, have focused
85 their attention on MQL technique owing to its benefits such as improved machining
86 performance, enhanced tool life, optimal use of MWF's, and effective heat dissipation from
87 cutting zone [4].

88 The MQL uses a mist spray of cutting fluid, which is more efficient than flood cooling [5].
89 Gupta et al. [6] examined and optimized the MQL aided turning of Inconel 718 with CBN
90 inserts. They observed that rise in the feed rate results in higher cutting forces while the material
91 removal rate (MRR) increases at higher cutting speed. The performance of MQL aided milling
92 of Inconel 718 has been compared with that of dry and flood assisted milling by Singh et al.
93 [7]. They claimed that MQL results in better machining performance reducing the cutting tool
94 flank wear related to flood and dry conditions. In other research, Uzun et al. [8] reported micro-
95 machining of Inconel 718 with different coated cutting tools in MQL assisted and dry
96 conditions. They claimed that coating materials have substantial influence on tool life and tool
97 wear at MQL environment.

98 Biodegradability is critically essential considering human health and the environment. For
99 meeting biodegradability, vegetable oils and esters, owing to their renewability, environment

100 friendly nature and less toxicity, are obvious choices to prepare cutting fluids [9]. Therefore,
101 use of vegetable oils as a MQL coolant has been also suggested in the literature [3, 10, 11].
102 Although, Obikawa et al. [12] reported that the MQL conditions are not always suitable for
103 better machining performance, especially when enormous heat produced during machining of
104 difficult-to-cut materials. Hence, an enhanced MQL fluid should be developed with higher
105 lubrication and cooling capacities. Such enhancement for MQL is possible with use of
106 nanofluids which have high thermal conductivity suitable for better heat dissipation during
107 cutting operation. Nanofluids are synthesized by dispersion of nanoparticles (size less than
108 100nm) in the base fluids such as esters, vegetable oils, synthetic oils, etc. This process
109 augments the thermo-physical properties of nanofluids suitable for effective heat transfer
110 medium [13]. Yi et al. [14] proposed that practice of graphene oxide nanofluids results in
111 reduced cutting temperatures and cutting forces at the cutting region during turning of
112 Ti6Al4V. They also noted that graphene oxide nanofluids yield increased lubrication and
113 reduced friction forces. Gaurav et al. [11] proposed sustainable machining of Ti6Al4V using
114 jajoba vegetable oil with and without molybdenum disulfide nano-particles ($n\text{MoS}_2$) for pure
115 MQL and NFMQL machining, respectively. They reported that addition of $n\text{MoS}_2$ based jajoba
116 oil significantly enhances the machining performance. Cui et al. [15] reported effects of the
117 biomimetic microstructure, the multi-walled carbon nanotubes based vegetable-oil nanofluid
118 MQL and their interaction attributes in minimizing the specific cutting energy and reduction
119 of emission of harmful gases during the machining.

120 However, the limiting factor for the use of nanofluid as coolant in machining operations could
121 be the improper stability in the base fluid [16]. Typically, various surfactants are mixed in base
122 fluid for uniform dispersion of nanoparticles to improve the stability. However, the use of
123 surfactants such as Tween20, Tween80 and sodium dodecyl sulfate (SDS) reduces the thermal
124 conductivity of the coolants and, hence, they are not the best suitable option for coolants where

125 cooling is a major job. Therefore, development of nanofluid with better a stability as well as
126 enhanced thermo-physical properties is important consideration.

127 Another important aspect in machining is to optimize the process performance whilst lessening
128 the negative effects on on health and environment. Thus, in this study, TGRA approach was
129 employed to find the optimal machining conditions for the multiple quality characteristics.
130 With application of TGRA, a mult-response optimization can be accomplished easily unlike
131 the traditional mono-optimization. Deng's TGRA approach typically used to quantify the
132 degree of approximation amid the sequences using the Grey Relational Grade. Lately, few
133 academics have successfully shown the application of TGRA approach for the multi-response
134 optimization improving the overall performance of the machining processes [17, 18].
135 Therefore, we employed TGRA for the multi-response optimization of face milling of Inconel
136 718 under different machining environments.

137 The literature review disclosed a need of synthesis of a nanofluid with better thermal
138 conductivity whilst retaining stability. Therefore, a hybrid nanofluid comprising of the silver
139 coated zinc oxide (Ag/ZnO) hybrid nanoparticles in ethylene glycol base has been proposed
140 for NFMQL application in this study. Initially, Ag/ZnO nanoparticles were synthesized and
141 characterized and then they were dispersed at different volume concentrations in base fluid.
142 Further, the prepared nanofluids were characterized for their thermo-physical properties viz.
143 zeta potential, effective thermal conductivity, and viscosity. Then, nanofluid with better
144 properties was chosen for NFMQL application. The machining performance of Inconel 718
145 was investigated under different machining conditions in terms of average surface roughness,
146 cutting temperature and tool wear. Finally, TGRA approach was implemented to find the best
147 machining conditions considering the multiple quality characteristics.

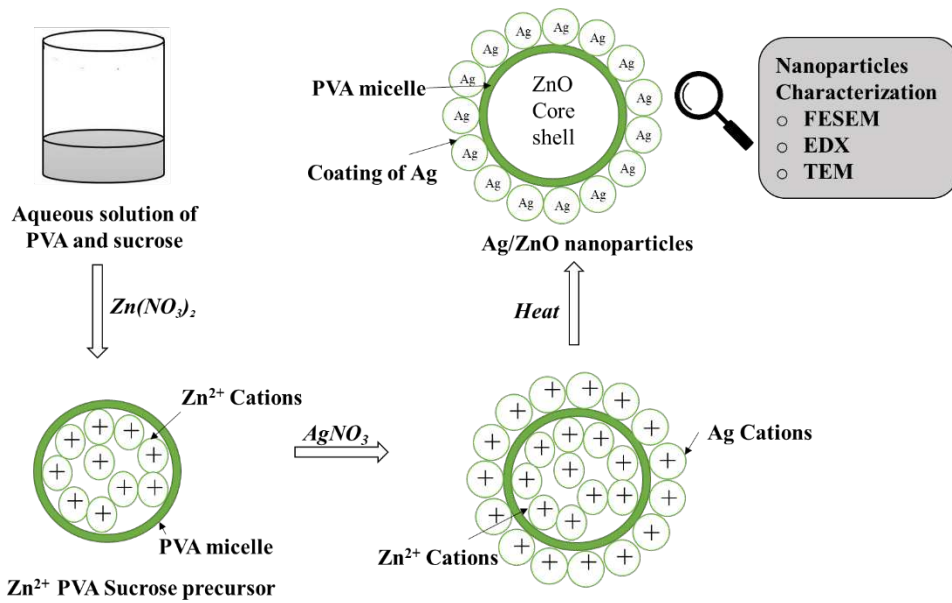
148 2. Experimentation

149 2.1 Preparation and characterization of hybrid nanofluids

150 The hybrid nanofluids were blended by two-step approach. Initially, the Ag/ZnO nanoparticles
151 were prepared by the chemical precursor process. The method for the synthesis of Ag/ZnO
152 nanoparticles is schematically represented in Fig. 1. The sole-gel chemical reaction of the PVA,
153 sucrose, zinc salt and Silver salt was carried out. A fine polymer-coated powder of zinc was
154 acquired by stirring the aqueous phase of PVA and sucrose at 24 hr. For a proper reaction, the
155 solution was heated to 65-75 °C and, concurrently, the zinc salt was added (pH ~9) to upkeep
156 hydrogenation of the Zn⁺ ions. These fine polymers coated zinc salt powder was then mixed in
157 the silver nitrate solution using magnetic stirring at 50-60 °C. Lastly, the acquired powder was
158 heated at 500-600 °C for 2 hours to obtain the recrystallized ZnO nanoparticles covered with a
159 steady thin shell coat of Ag. The primary purpose of this defined shape nanoparticles synthesis
160 was to attain the Ag coated ZnO nanoparticle for taking benefit of both the characteristics of
161 the nanoparticles and the achievement of the stable nanofluid suitable for use in the MQL
162 process. Such synthesis can realise the nanoparticles up to size of 20 nm [19].

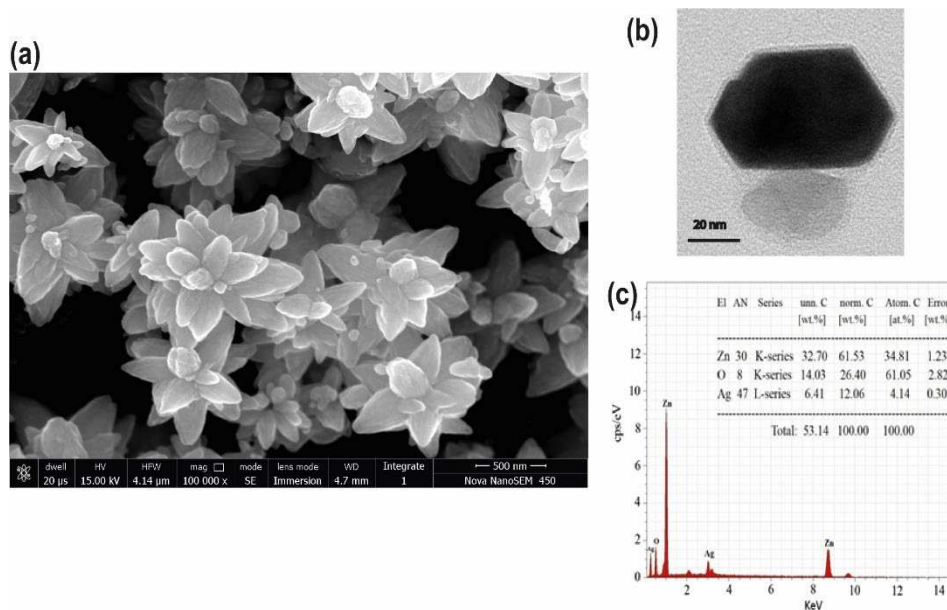
163 The surface morphology of the synthesized nanoparticles was confirmed by the FESEM (Carl
164 Zeiss® SUPRA 55) images. The clusters of Ag/ZnO nanoparticles in flower petal structure can
165 be observed in Fig. 2(a). These clusters are in the range of 500 nm - 1 µm containing 25-30
166 nanoparticles. A closer view of Ag/ZnO nanoparticles shown in Fig. 2(b) by a high-resolution
167 tunneling electron microscope (TEM). This TEM image of the Ag/ZnO nanoparticle confirms
168 the size of the nanoparticles in the order of 20-50 nm. The individual elemental constituent in
169 the synthesized Ag/ZnO nanoparticle examined by energy dispersive x-ray (EDX) analysis.
170 Fig. 2(c) verifies the occurrence of zinc, oxygen and silver in 34.81 %, 61.05 %, and 4.14 %,
171 respectively. The synthesized hybrid nanoparticles had the Wurtzite crystal structure
172 surrounded by flower petals with density of 6.24 gm/cm³, and appeared in gray color. The

173 detailed characterization representing the structural and electrical properties of the Ag/ZnO
 174 particles has been reported by our colleagues Jadhav and Biswas [19].



175
 176
 177

Fig. 1. Graphical representation of production of Ag/ZnO Hybrid nanoparticles.



178 **Fig. 2.** Characterisation of Ag/ZnO nanoparticles, (a) FESEM image showing the hexagonal
 179 clusters Ag/ZnO nanoparticles, (b) TEM image, (c) EDX spectrum.

180 In the second step, these synthesized nanoparticles were dispersed in the ethylene glycol at
 181 volume concentration varied between 0.05 %, 0.10 %, 0.15 %, and 0.2 % (Eq. 1).

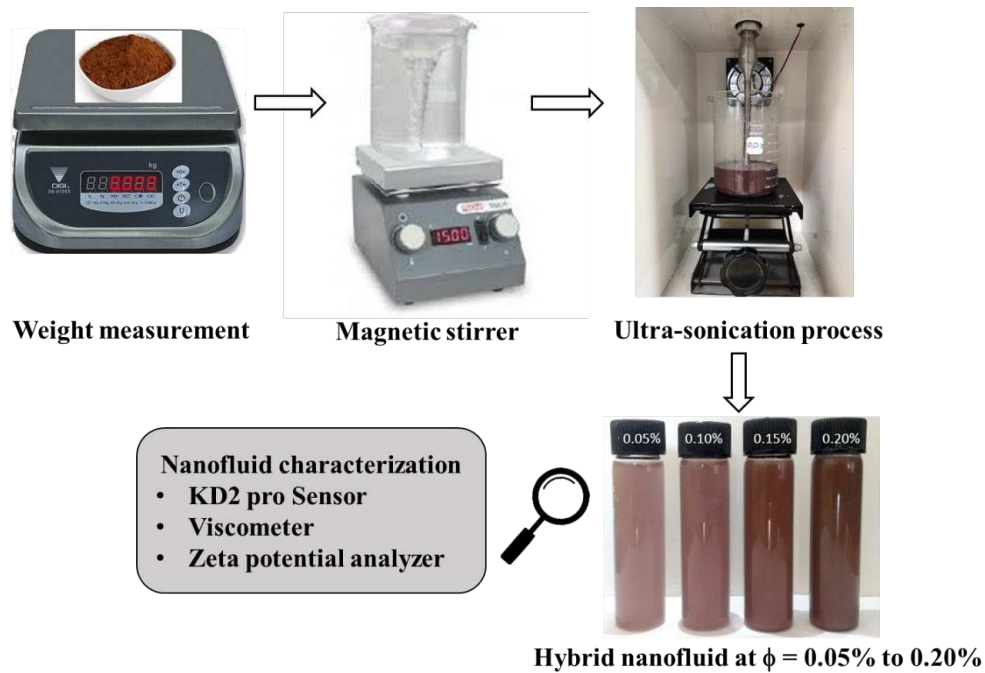
$$\phi = \frac{\frac{m_{hn}}{\rho_{hn}}}{\frac{m_{bf}}{\rho_{bf}} + \frac{m_{hn}}{\rho_{hn}}} \quad (1)$$

182 The thermo-physical characteristics of ethylene glycol are depicted in Table 1.

183 **Table 1** Properties of the ethylene glycol.

Property	Value
Flash point	111 °C
Viscosity	1.61×10^{-2} Pa·s
Density	1.11 gm/cm ³
Thermal conductivity	0.252 W/m ² -K

184 The stability is an important parameter to decide the nanofluids thermo-physical properties. To
 185 accomplish a stable dispersion of the nanoparticles, the prepared nanofluid was agitated by
 186 magnetic stirring and then ultrasonicated for 1 hour (see, Fig. 3). The nanofluid stability
 187 characterization was carried out by the two ways, namely, visual observation and by measuring
 188 the zeta potential values using (Malvern Instrument®, Nano-ZS).



189

190 **Fig. 3.** Schematic procedure of synthesis of glycol-based Ag/ZnO hybrid nanofluid.

191 The prepared nanofluids at different concentrations of nanoparticles were examined for their
192 thermo-physical properties viz. the thermal conductivity and dynamic viscosity at different
193 temperatures. The thermal conductivity was measured by KD2 pro sensor because of its higher
194 accuracy [20]. The viscosity of the prepared nanofluid was determined with the cone and plate
195 viscometer.

196 **2.2 Workpiece, tool and CNC milling with MQL setup**

197 For the current research, commercially available Inconel 718 material was used and cut into
198 plates of size 120 X10 X 6 mm. A 12 mm diameter indexable cutter (Secotools® R217.69-
199 1212.0-06-2AN) purchased from Seco tools India Limited. The milling inserts (Secotools®
200 XOMX060204R-M05 F40 M; clearance angle 15°, effective cutting edge length 5.5 mm,
201 corner radius 0.40 mm, insert width 4.1 mm) used were coated grade carbide inserts with TiAlN
202 coating obtained by the physical vapor deposition coating method. The TiAlN coating offers a
203 better wear-resistant and reduced friction while machining difficult-to-cut materials. New
204 inserts were used for each experimental run. Experimental runs were performed on the MTAB
205 Maxmill+ vertical machining centre having X, Y and Z drives with limits as 480 mm, 360 mm
206 and 500 mm, respectively, and with the accuracy of 0.01 mm. The Siemens 828D controller
207 is equipped on the machine for programming and operations. An MQL setup was utilized which
208 had external MQL nozzle to spray cutting fluid directly into the cutting region. The angle of
209 jet with respect to tool axis was 45° and the distance between nozzle and tool face was kept 60
210 mm. This distance was selected such that the jet covers the entire face of cutting tool. The air
211 pressure of 6 bar and flow rate of 35 ml/hr was selected for MQL spraying considered from the
212 literature [7, 21].

2.3 Milling Experiments

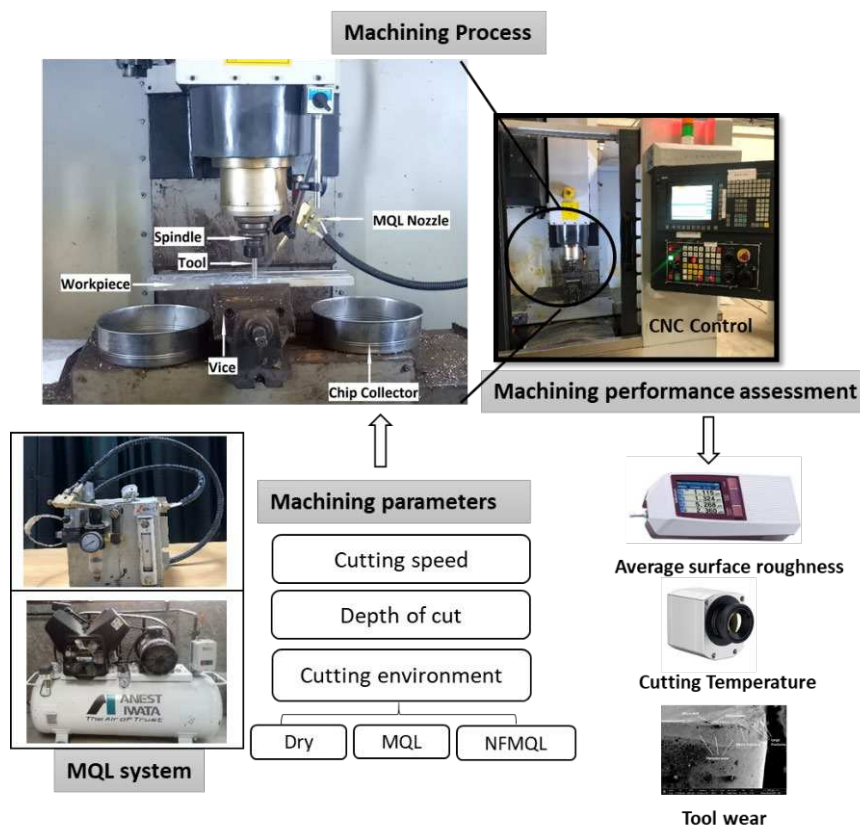
The milling of Inconel 718 was performed varying three input machining parameters, namely, cutting speed, feed/tooth and cooling environment. The major goal of the work was to compare the effect of NFMQL environment with other cutting environments; therefore, cutting environment was selected as input parameter. Three cooling conditions were selected viz. dry, MQL and NFMQL. The dry condition involves milling without any coolant, while ethylene glycol was chosen as cutting fluid for MQL flow cooling conditions. For NFMQL, the nanofluid with the best properties was selected out of the prepared nanofluids. The three input parameters by considering three levels of each were chosen, as revealed in Table 2. Taguchi methodology is extensively used to design experiments, especially in the manufacturing domain. The orthogonal array-based designs provide an efficient approach to evaluate the effect of process factors on response variables and deliver optimum setting of factors impervious to noise. Taguchi L9 orthogonal array was chosen to accommodate these input factors and plan the experiments. The milling performance was analyzed in terms of average surface roughness and cutting temperature.

Table 2 Machining parameters and their levels.

Parameter	Level 1	Level 2	Level 3
Cutting speed (m/min)	30	45	60
Feed/tooth (mm/min)	0.036	0.046	0.056
Cooling environment	Dry	MQL	NFMQL

The average surface roughness (R_a) of the surface prior and after machining was analyzed using the surface roughness profilometer (Mitutoyo® SJ-210). The profilometer contained a diamond stylus connected to its probe which moves over the surface to trace the crest and troughs of the surface. The conformance standard of the profilometer was ISO-1997 with filter-gauss. The

233 measurements were performed with a sampling length of 0.8 mm, an evaluation length of 4mm
 234 and travel length of 4.8 mm, and the running at a speed of 0.5 mm/min with diamond stylus.
 235 R_a measurements were performed at five locations on the workpiece and the mean value was
 236 considered for further analysis in this paper. The maximum cutting temperature was measured
 237 using an infrared camera (Optris® PI 400i) set to measure temperature range between 0 to
 238 800°C. The insert wear was observed using images taken by FESEM. The schematic of
 239 experimental setup is presented in Fig. 4.



240

241

Fig. 4. Schematic of CNC milling experiments.

242

3. Results and discussion

243

3.1 Characterization and selection of nanofluids

244

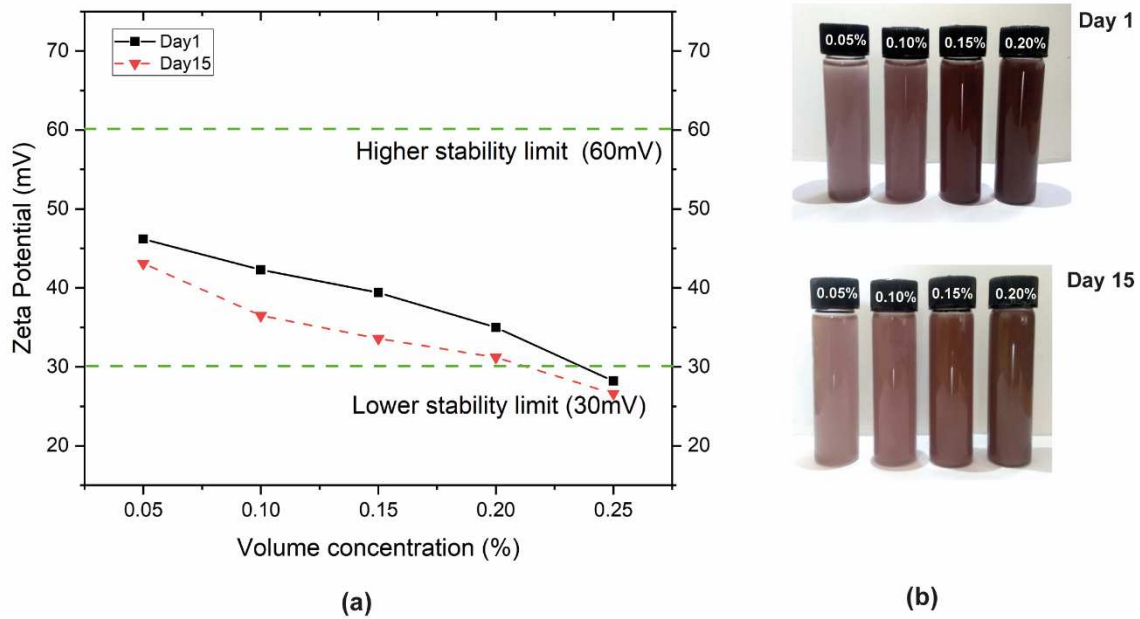
As described previously, the nanofluids with numerous concentrations (viz. 0.05%, 0.10%,

245

0.15%, and 0.2%) by volume of hybrid nanoparticles were prepared and then their thermo-

246 physical properties were characterized for selection of nanofluid with best properties for
247 NFMQL based milling tests.

248 For the stability measurement, the visual tests were carried out by observing the prepared
249 nanofluids for possible sedimentation/agglomeration of the nanoparticles. The
250 sedimentation/agglomeration of nanoparticles at the bottom of flasks was not found until 15
251 days for all nanofluids (see Fig. 5). Therefore, the prepared nanofluids considered to be having
252 good stability. The measurement of zeta potential values, referred to as the repulsive forces
253 between particles is another essential aspect to highlight the stability of such nanofluids [22].
254 The stability of prepared nanofluids was analyzed in terms of zeta potential values and visual
255 observations recorded at day 1 and day 15 (see, Fig. 5). According to the stabilization theory,
256 the agglomeration of nanoparticles is inversely proportional to the electrostatic repulsion in
257 particles and higher electrostatic repulsion typically observed for high zeta potential values. It
258 is stated that nanofluids that have absolute zeta potential values between 30 to 60 mV are very
259 stable. Fig. 5 (a) shows the zeta potential values for prepared nanofluids measured at room
260 temperature (25 °C). Although the zeta potential values declined with a rise in nanoparticle
261 concentration, the zeta potential values were well in within the range of 30 to 60 mV (range for
262 higher stability) $\Phi = 0.05\%$ to 0.2% . But for the 0.25% volume concentration, the zeta
263 potential value dropped below 30 mV. Therefore, according to the zeta potential tests and visual
264 observations (Fig. 7 (b)), the prepared nanofluids with a volume concentration between $\Phi =$
265 0.05% to 0.2% were perceived to be stable and having good dispersion characteristics. Thus,
266 the nanofluids with volume concentration 0.05% to 0.20% were selected for further
267 characterization.



268

269 **Fig. 5.** Stability investigation of hybrid nanofluids at different concentrations (a) zeta

270

potential, (b) photographs.

271

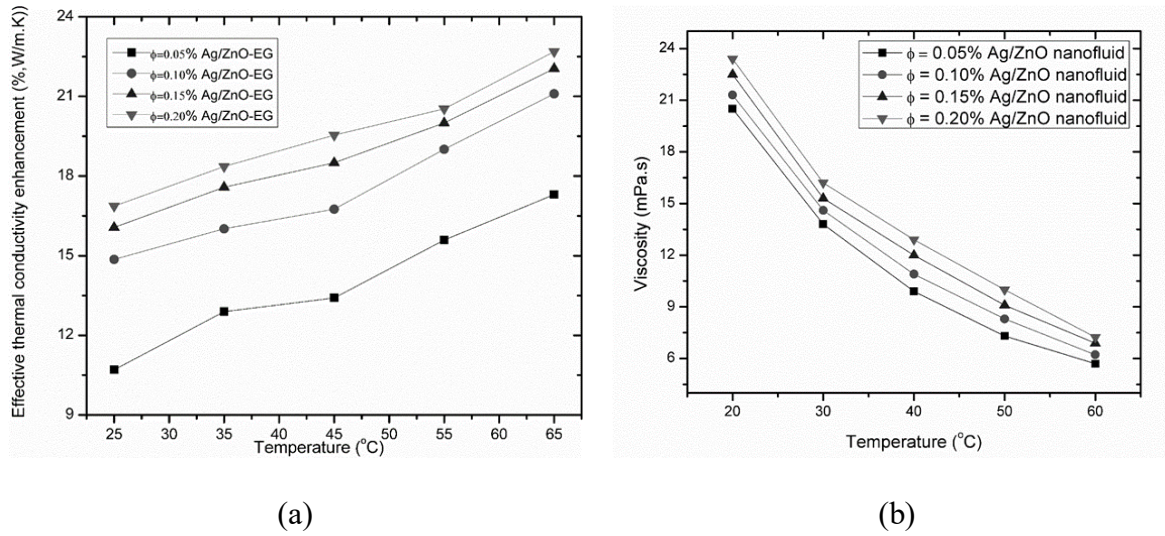
The thermal conductivity of synthesized nanofluids was analysed with KD2 sensor. The accuracy of $\pm 2\%$ was quantified for the measurement of thermal conductivities of DI water and ethylene glycol. Then, the thermal conductivity of the prepared nanofluids was measured at varying temperature ranging from 25 to 65 °C (Fig. 9). An increased thermal conductivity was seen for increasing the values of the concentration of nanoparticles and temperature. It is found that for 0.20% volume concentration of nanoparticle, the maximum 15% enhancement in thermal conductivity compared with ethylene glycol at 25 °C was recorded. High thermal conductivity yields improved Brownian motion of the nanoparticles that increases the lattice vibration between the molecules.

280

Similarly, the viscosity of fluids was appeared to be increasing with an increase in concentrations of nanoparticles. It is appreciated that viscosity value of nanofluid drops with a rise in temperature, but this decrement is marginal compared with viscosity of the glycol (see, Fig. 6). The fluid with higher viscosity and higher thermal conductivity generally well suited

283

284 as coolant in machining operations. Therefore, the hybrid nanofluid with 0.2% concentration
 285 of Ag/ZnO was selected as a coolant for NFMQL operation in further study.



286 **Fig. 6.** Properties of hybrid nanofluid at different temperature, (a) effective thermal
 287 conductivity, (b) dynamic viscosity of the hybrid nanofluid at different temperature.

288 3.2 Effect of process parameters on responses

289 As discussed previously, the milling experiments were planned via Taguchi L9 orthogonal
 290 array. Table 3 displays the experimental runs and measured response values and S/N ratio
 291 values for response variables. To assess the effect of input machining parameters on response
 292 variables, lower-the-better S/N ratio criteria was used. The lower values of R_a and cutting
 293 temperature demonstrates the better machining performance. Therefore, lower-the-better
 294 criteria was used to calculate the S/N ratios. Higher the S/N ratio typically correspond to
 295 optimum value of input factor to yield better process performance. The S/N ratio values for
 296 both responses were determined using following equation.

$$297 \quad \frac{S}{N}(\eta) = -10 \log \left[\frac{1}{9} \sum_{i=1}^9 y_i^2 \right] \quad (2)$$

298 Where, y_i is the measured value of response for i th run.

299 In the following sections, the effects of input factors on response variables have been discussed.

Table 3 Effect of machining factors on the responses.

Run	Input machining parameters			Response variables			
	Cutting speed (m/min)	Feed rate (mm/tooth)	Cutting environment	Average surface roughness (μm)		Cutting temperature ($^{\circ}\text{C}$)	
				Mean Value	R_a S/N ratio (dB)	Value	S/N ratio (dB)
1	30	0.036	Dry	2.26	-7.082	238	-47.531
2	30	0.046	MQL	2.37	-7.495	245	-47.783
3	30	0.056	NFMQL	2.15	-6.649	223	-46.966
4	45	0.036	MQL	1.68	-4.506	248	-47.889
5	45	0.046	NFMQL	1.61	-4.136	238	-47.531
6	45	0.056	DRY	2.35	-7.421	290	-49.248
7	60	0.036	NFMQL	1.11	-0.906	244	-47.748
8	60	0.046	DRY	1.75	-4.861	305	-49.686
9	60	0.056	MQL	1.55	-3.807	278	-48.881

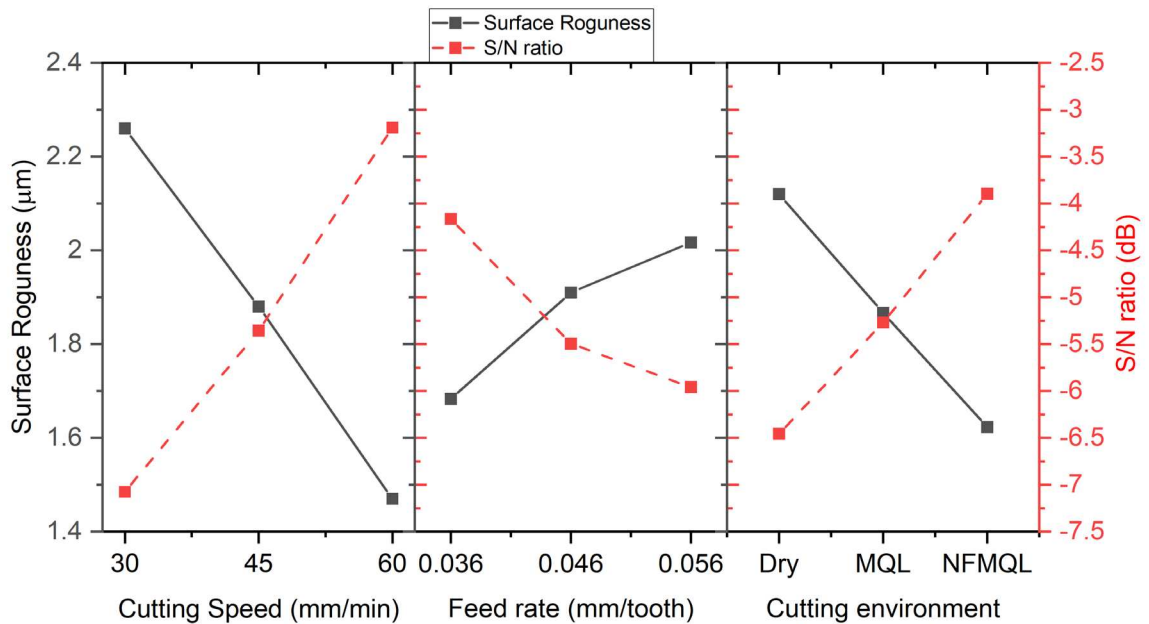
3.2.1 Average surface roughness (R_a)

The impact of cutting speed, feed/tooth and cooling environment on the average surface roughness values is depicted in Fig. 7. It is clear that the dry machining associated with the poorest surface finish, while MQL and NFMQL reduced the R_a value significantly. In absence of the cooling and lubrication, tool undergoes the adhesion wear resulting in the high temperature and stresses at tool tip [23]. The lowest R_a was witnessed at NFMQL having 20 % hybrid Ag/ZnO nanoparticles. The introduction of cooling and lubrication is known for enhancing the surface finish while machining operations [17]. Although, usage of nanofluid in

309 MQL yielded better surface finish than MQL owing to its better thermo-physical properties. It
310 was found that NFMQL improves the surface finish by 23.5 % and 13.07 % as related to dry
311 and MQL cooling environments, respectively. The NFMQL attributes the adequate lubrication
312 and heat withdrawal from the machining zone, thus, leading to a positive impact on surface finish. The
313 nanoparticles could avoid the welding of chips on inserts and owing to the ball-bearing effect of
314 nanoparticles, the chips slide easily over the tool surface. Generally, the surface roughness
315 depends on feed rate and nose radius, and with a rise in feed/tooth the R_a rises as seen from
316 Fig. 7. The mean value of surface roughness at 0.036 mm/min of feed/tooth is 1.683 μm which
317 increased by 13.5 % to 1.91 μm and by 19.84 % to 2.017 μm at feed/tooth of 0.046 and 0.056,
318 respectively. At high cutting speed, the R_a values were observed to be reducing. Such a trend of
319 decrease of surface roughness with an increase in cutting speed can be explained by considering
320 the role of vibration at low cutting speed. At low cutting speed, the machine may experience vibration,
321 especially while cutting difficult-to-cut superalloys and hard materials, since the workpiece
322 material is not adequately warm to result in material softening. Higher cutting speeds result
323 in high cutting temperatures which allow easy deformation of the workpiece without being
324 torn, thus improving the surface finish [24]. Contrarily, the higher cutting speed decreases the
325 vibration and chatter effects, and as a result, the R_a decreases. Further, with an increase in
326 cutting speed, the required cutting force for cutting action decreases. Similar trends of decrease
327 of R_a with an increase in cutting speed value up to 60 m/min were also reported by Mia et al.
328 [25]. They reported that when the cutting speed rises further above 60 mm/min, it results in
329 increased R_a values due to larger stickiness (i.e. adhesion) of the workpiece and formation of built-
330 up-edge (BUE).

331 The S/N ratio trend for different input factor settings can be seen from Fig. 7. According to
332 S/N ratio analysis, the higher S/N ratio is desirable for optimum setting of input parameters.
333 The optimum machining performance to yield lower surface roughness can be realized at

334 cutting speed of 60 m/min (level 3), feed rate of 0.036 mm/tooth (level 1), and with NFMQL
 335 cutting environment (level 3). In other words, the higher cutting speed, lower feed rate and
 336 NFMQL cooling environment are ideal for achieving the better surface finish while milling of
 337 Inconel 718.



338

339 **Fig. 7.** Effect of machining factors on the surface roughness.

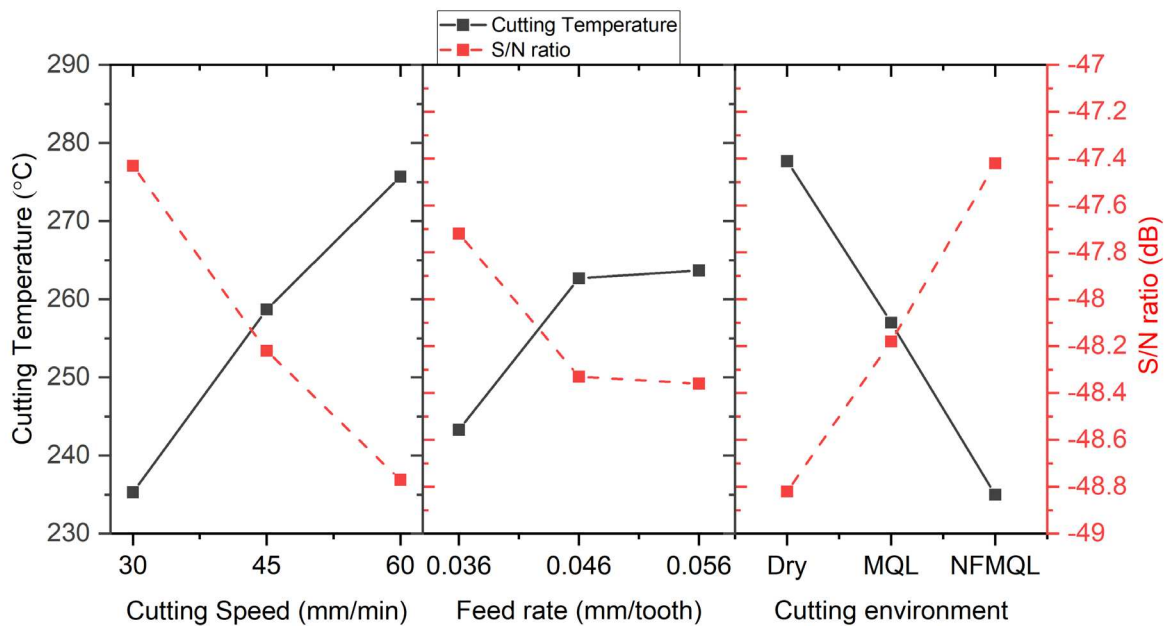
340 3.2.2 Cutting temperature

341 The cutting temperature often considered as a major factor in the machining process as it
 342 influence the tool wear, dimensional accuracy surface integrity, etc. The influence of cutting
 343 speed, feed/tooth and cutting environment on cutting temperature is shown in Fig. 8. Higher
 344 cutting speed and feed rate are known for increasing the cutting temperature (see, Fig. 8).
 345 Higher the cutting speed, higher is the kinetic energy. Such large kinetic energy results in the
 346 tremendous heat generation in cutting region owing to plastic deformation at primary
 347 deformation region and friction at tool-chip zone and tool-work zone [25]. Although high
 348 cutting speed generally results in increased cutting temperatures, it is pre-requisite for increased
 349 productivity to ensure cleaner productions. Thus, the use of cutting fluids becomes a prime
 350 requirement for lowering the cutting temperature and increasing productivity. Similarly, with

351 an increase in feed/tooth value, cutting temperature seen to be increasing. It can be realized
352 from Fig. 8 that the highest heat liberated at dry cutting environment while machining Inconel
353 718. Whereas, the lowest temperature, i.e. better heat dissipation, resulted in NFMQL cooling
354 condition as compared to MQL condition. During dry machining, in the absence of cooling
355 medium, heat dissipation is very poor and therefore, high temperatures can be observed in the
356 cutting zone. The introduction of coolant fluid using MQL and NFMQL has a noteworthy effect
357 on reducing the cutting temperature. The mist and air in MQL take out the convective heat
358 transfer, while, the heat absorbed by ethylene glycol, which used as base fluid in MQL, results
359 in both convective and evaporative heat transfer. The NFMQL cutting environment reduced
360 the cutting temperature by 15.38 % and 8.56 % as compared to dry and MQL condition,
361 respectively. The nanofluid with 0.2 % hybrid Ag/ZnO nanoparticles had significant
362 enhancement in thermal conductivity owing to the high heat absorption ability of Ag/ZnO
363 nanoparticles. Moreover, as described previously, nanoparticles improve the lubrication and
364 helps in chips removal due to ball bearing effect. Thus, at NFMQL cooling, the heat dissipation
365 in even faster and reduces the cutting zone temperature. Similar results regarding reduced
366 cutting temperature with use of nanofluids during various machining operations are reported
367 in [26, 27]. Su et al. [27] reported that the graphite-LB2000 NFMQL had a better performance
368 than that of MQL and dry conditions and reduced the cutting temperature significantly. The
369 lowest cutting temperature was observed while using hBN nanoparticles based NFMQL as
370 compared to that of MQL and dry conditions by Yıldırım et al. [26]. They reported the
371 reduction of the cutting temperature by 30% compared to dry machining.

372 The optimum parametric settings suggested by S/N ratio analysis for lowest cutting
373 temperature are cutting speed of 30 m/min (level 1), feed rate of 0.036 mm/tooth (level 1), and
374 NFMQL cutting environment (level 3). Hence, to achieve a lower cutting temperature, low

375 cutting speed, low feed rate and NFMQL environment settings found to be best input
 376 conditions.



377

378

Fig. 8. Mean effect plot for cutting temperature.

379 **3.2.3 Analysis of variance (ANOVA)**

380 The statistical performance of the factors was assessed using the ANOVA at 95% confidence
 381 level and outcomes are depicted in Table 4. F values of the control factors indicated the
 382 significance of control factors with ANOVA analysis. P values less than 0.05 indicates whether
 383 the input factor has significant contribution on the response or not. As expected for milling
 384 operation, the cutting speed witnessed to be most significant factor for R_a contributing by 62.06
 385 %. The feed rate and cutting environments contributes on R_a by 11.52 % and 24.52 %, respectively.
 386 The cutting temperature was affected by the cutting speed and feed/tooth by 40.30
 387 % and 12.91 %, respectively. Both the cutting speed as well as the cutting environment found
 388 be having significant effect on response variable since their corresponding P values are less than
 389 0.05.

390

Table 4 ANOVA for surface roughness and cutting temperature

Factors	Degree of freedom	Sum of squares	Mean squares	F	P	Percentage contribution %
<u>Surface roughness</u>						
Cutting Speed	2	0.9366	0.46830	32.90	0.029	62.06%
Feed Rate	2	0.1738	0.08693	6.11	0.141	11.52%
Cutting Environment	2	0.3701	0.18503	13.00	0.071	24.52%
Error	2	0.02847	0.01423			
Total	8	1.50907				
<u>Cutting temperature</u>						
Cutting Speed	2	2460.2	1230.11	19.81	0.048	40.30%
Feed Rate	2	788.2	394.11	6.35	0.136	12.91%
Cutting Environment	2	2731.6	1365.78	21.99	0.043	44.74%
Error	2	124.2	62.11			
Total	8	6104.2				

391 **3.3 Effect of cutting environment on the tool wear**

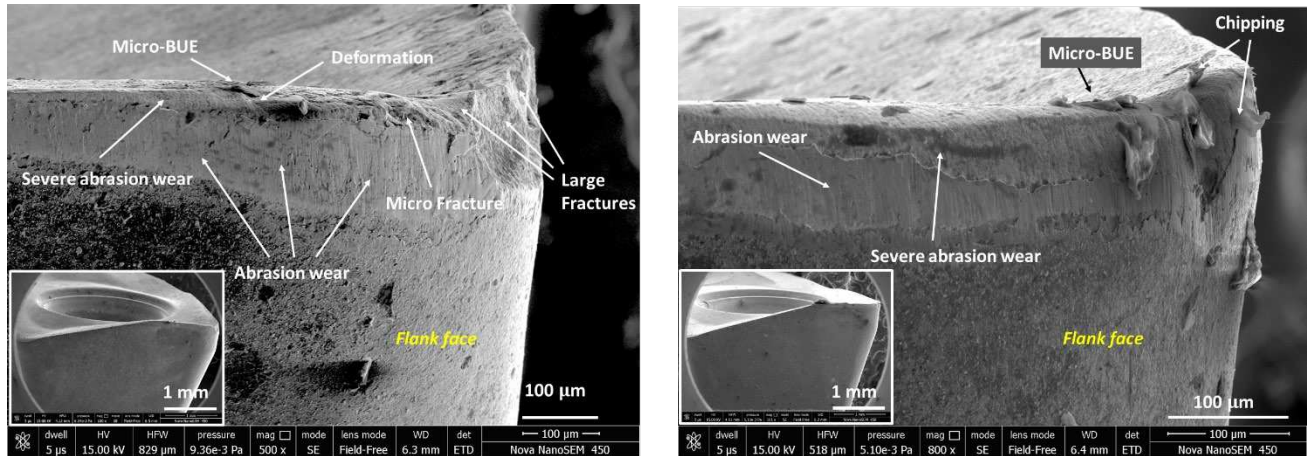
392 To investigate the influence of cooling/lubrication environment on tool wear, three additional
393 experiments were conducted while milling difficult-to-cut Inconel 718 workpiece at dry, MQL
394 and NFMQL conditions at a constant cutting speed of 60 m/min and feed/tooth of 0.06 mm/min.
395 The microscopic images of inserts after dry, MQL and NFMQL milling captured using a
396 scanning electron microscope are shown in Fig. 9 (a), (b), and (c), respectively.

397 A worse tool wear was witnessed for dry machining environment. The insert used in dry
398 machining undergone deformation, microfractures, abrasive wear, and micro built-up-edge

399 (BUE) formation. Similar observations were also reported in [28, 29]. Inconel 718 is hard and
400 sticky superalloy and, often, its machining results in work hardening resulting in excessive
401 stresses on cutting edges. At high cutting speed and feed values under dry environment, specific
402 cutting energy and high friction leads to enormous heat liberation and, thus, cutting insert
403 undergoes high tool wear. Under the application of MQL, NFMQL cooling environment, the
404 insert wear was found to significantly less than that of dry conditions as seen from Fig. 9. In
405 MQL, a little quantity of base oil is sprayed in the mist form, into the cutting region with the
406 using compressed air, forming a thin oil film at tool-workpiece and tool-chip zone and reduces
407 friction preventing the accumulation of heat. Moreover, the lubricating substance in MQL
408 allows to pass away the heat produced due to friction at cutting tool. This decreases the tool
409 wear also increases the tool life.

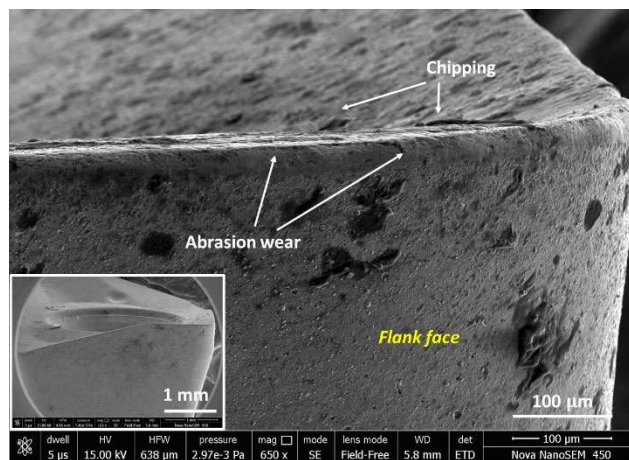
410 The MQL method is eco-friendly and safe for users if used with appropriate coolant which is
411 desired in this study. The chips from MQL are non-corroded and recycled. Among the MQL
412 and NFMQL, the least amount of wear was observed in NFMQL as demonstrated in Fig. 9 (b)
413 and (c). Hybrid nanofluid consisting of Ag/ZnO nanoparticles shows a better effect due to its
414 ability of high heat extraction from the cutting region. Similar observation regarding ability of
415 nanofluid for enhanced heat extraction has been reported by Yildırım et al. [26]. The best
416 surface finish witnessed in NFMQL condition while the poor surface quality was observed in
417 dry machining.

418 These preliminary experimental results show that the proposed hybrid Ag/ZnO nanofluid is
419 superior for NFMQL application during milling of Inconel 718. However, an extensive
420 experimental work is required to be done to critically examine the performance of proposed
421 nanofluid at different concentration and cutting conditions. Further, study of the physics of
422 droplet interaction, the surface chemical characterization after machining, etc. is required to to
423 explain the action mechanism illustrating benefits of proposed hybrid nanofluid.



(a) dry

(b) MQL



(c) NFMQL

424 **Fig. 9.** FESEM images for tool wear at different cutting environment (a) Dry, (b) MQL, (c)
 425 NFMQL; (at cutting speed of 60 m/min and feed/tooth of 0.06 mm/min).

426 3.4 Taguchi grey relational analysis based multi-response optimization

427 In previous sections, the signal-to-noise (S/N) ratio analysis was used to determine the
 428 optimum sets of factors in single objective optimization for minimizing the average surface
 429 roughness and cutting temperature, separately. However, such approach is not suitable for
 430 multi-response optimization cases such as in the current work. Therefore, TGRA was applied
 431 for simultaneous optimization of the average surface roughness and cutting temperature.
 432 Initially, the grey relational generating based on “smaller the better” criteria was employed to
 433 normalise the measured response values since smaller surface roughness and cutting

434 temperature are desirable characteristics [30]. The grey relational generating on “smaller the
 435 better” was accomplished through following equation:

$$436 \quad x_{ij} = \frac{\max_j y_{ij} - y_{ij}}{\max_j y_{ij} - \min_j y_{ij}} \quad (3)$$

437 Where, y_{ij} for the i^{th} experimental result in the j^{th} experiment.

438 Generally, the greater normalized values signify an enhanced performance, and the best
 439 normalized value should be unity. Subsequently, the grey relation coefficients were determined
 440 to describe the correlation between the best and the normalized response values. The grey
 441 relation coefficient was calculated using following equation,

$$442 \quad \xi_{ij} = \frac{\min_i \min_j |x_i^0 - x_{ij}| + \zeta \max_i \max_j |x_i^0 - x_{ij}|}{|x_i^0 - x_{ij}| + \zeta \max_i \max_j |x_i^0 - x_{ij}|} \quad (4)$$

443 where x_i^0 is the best normalized value for the i^{th} response variable and ζ is the distinctive
 444 constant (here, assumed to be 0.5) which is defined in the range $0 \leq \zeta \leq 1$.

445 Finally, the grey relation grade (GRG) was determined by taking an average of the grey
 446 relation coefficient for respective response variable. The GRG value was determined using
 447 equation (5).

$$448 \quad \gamma_j = \frac{1}{m} \sum_{i=1}^m \xi_{ij} \quad (5)$$

449 where γ_j is the GRG of the j^{th} trial and ‘ m ’ is the number of response variables (here, $m=2$).

450 Table 5 lists the calculated values of normalised input factors, grey relational coefficients and
 451 the GRG. The GRG values have been ordered from high to small value to decide their rank.

452 The last column of Table 5 represents the calculated GRG values and the order in which it

453 was ranked from high value to small. A higher value of the GRG exhibits the better

454 performance of outputs for all results simultaneously. The experimental run 6 is marked as 1

455 and the combination of input factors for this run is the best possible combination of factors

456 among the all runs. Therefore, the cutting speed of 30 mm/min, feed rate of 0.036 mm/tooth,
 457 and NFMQL cutting environment is the best combination showing the optimum parameters
 458 for multi-response optimization in the current experimental design. Since, a higher value of
 459 the GRG exhibits the better machining performance, therefore, the larger-the-better S/N ratio
 460 was used to find the optimal experimental run for the multi-response optimization. Larger-
 461 the-better criteria for higher GRG is defined as follows:

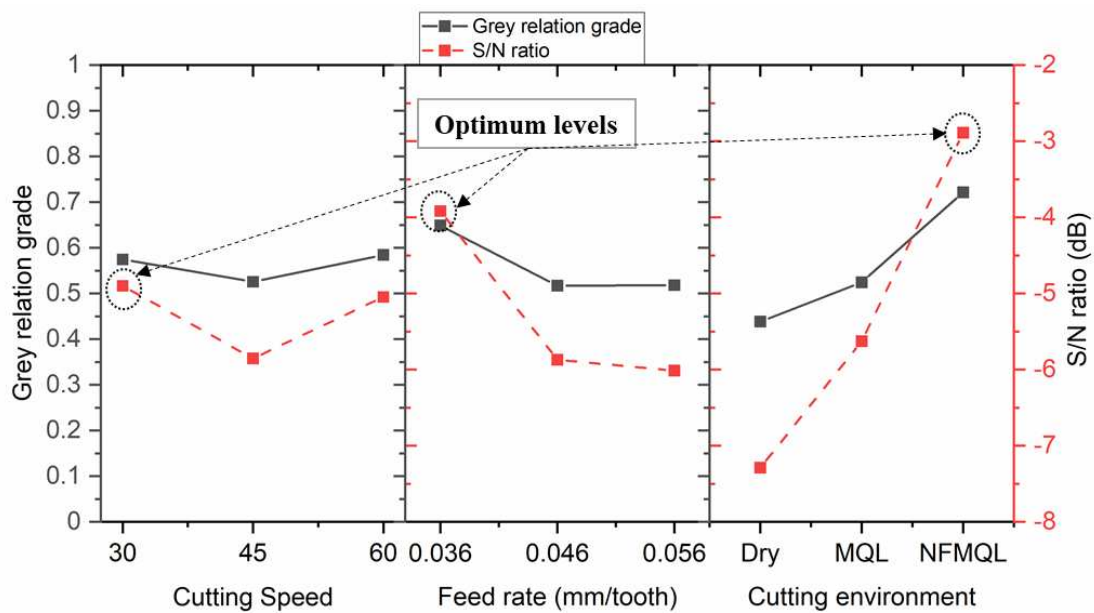
$$462 \quad \frac{S}{N}(\eta) = -10 \log_{10} \left[\frac{1}{9} \sum_{i=1}^9 \frac{1}{y_i^2} \right] \quad (6)$$

463 Where, y_i is the GRG value of response for i th run. In order to determine the effect of each
 464 level, the mean value of GRG and S/N ratios for GRG were calculated for the multiple
 465 quality characteristics are plotted in Fig. 10. The highest level of each factor directs the
 466 optimum level for that factor. In addition, the parameter with the highest difference between
 467 the maximum value and minimum value is the most contributing factor on gray relation
 468 grade. As seen from Fig. 10, the highest S/N ratio of GRG corresponds to optimum levels of
 469 machining factors are obtained as cutting speed at level 1 (30 mm/min), feed rate at level 1
 470 (0.036 mm/tooth), and cutting environment at level 3 (NFMQL). The highest difference
 471 between the maximum value and minimum value of GRG was recorded for the cutting
 472 environment, the cutting environment is the as the most dominant factor following by feed
 473 rate and then cutting speed for multi-response characteristics.

474 **Table 5** TGRA based grey relational generation, grey relational coefficient and grey
 475 relational grade.

Expt. No.	Normalised values of response variables		Grey relational coefficient		Grey relational grade	
	Surface roughness	Cutting Temperature	Surface roughness	Cutting Temperature	Value	Rank

1	0.08730	0.817073	0.35393	0.73214	0.54304	5
2	0.00000	0.731707	0.33333	0.65079	0.49206	7
3	0.17460	1.00000	0.37725	1.00000	0.68862	2
4	0.54762	0.695122	0.52500	0.62121	0.57311	4
5	0.60317	0.817073	0.55752	0.73214	0.64483	3
6	0.01587	0.182927	0.33690	0.37963	0.35826	9
7	1.00000	0.743902	1.00000	0.66129	0.83065	1
8	0.49206	0.00000	0.49606	0.33333	0.41470	8
9	0.65079	0.329268	0.58879	0.42708	0.50793	6



476

477

Fig. 10. Effect of machining input factors on the grey relation grade.

478

3.4.1 ANOVA analysis of GRG

479

ANOVA was applied to check the effect of input factors on the multi-response variables. The

480

outcomes of ANOVA listed in Table 6 directed that the cutting speed, feed rate, and cutting

481

environment significantly contributes ($P < 0.05$) deciding the GRG values by 3.60 %, 20.67 %

482 and 75.67 %, respectively. Interestingly, the cutting environment found to be the most
 483 substantial parameter governing the multiple performance characteristics and contributes by
 484 75.67 %, suggesting a positive impact on multiresponse machining characteristics. Thus, it can
 485 be claimed that NFMQL assisted milling is appropriate to improve the surface finish whilst
 486 reducing the cutting temperature. The proposed hybrid nanofluid found suitable for cleaner
 487 production in the machining domain.

488 **Table 6** ANOVA for GRG.

Factors	Degree of freedom	Sum of squares	Mean of squares	F	P	Percentage contribution %
Cutting Speed	2	0.005999	0.003000	87.63	0.011	3.60%
Feed Rate	2	0.034425	0.017213	502.86	0.002	20.67%
Cutting Environment	2	0.126073	0.063036	1841.59	0.001	75.67%
Error	2	0.000068	0.000034			
Total	8	0.166566				

489 **3.4.2 Confirmation experiments**

490 Finally, the confirmation experiments were performed at optimal level of input factors to
 491 confirm the improvement in the responses variables. The estimated GRG at optimal set of input
 492 factors can be computed by following equation [30]:

$$493 \quad \hat{\alpha} = \alpha_m + \sum_{i=1}^q \bar{\alpha}_i - \alpha_m \quad \dots (7)$$

494 here α_m = is the total mean of the GRG, $\bar{\alpha}_i$ is the mean of the GRG at the optimal level, and q
 495 is the number of the input factors that significantly affects the multiple response variables.

496 Table 7 shows a good agreement between the estimated GRG and experimental GRG obtained
 497 at optimum levels of input factors. Further, a percentage improvement of 25.04 % in GRG from
 498 initial factor setting (V_c-2 F_r-2 , CE-3) to optimum factors setting (V_c-1 F_r-1 , CE-3) was
 499 observed. Therefore, the current optimization results are claimed to be satisfactory and thus,
 500 improving the milling performance of Inconel 718.

501 **Table 7** Results of machining performance using initial and optimal machining parameter.

Machining Parameters	Initial	machining	Optimum machining parameters	
	parameters		Predicted	Experimental
	V_c-2 F_r-2 , CE-3		V_c-1 F_r-1 , CE-3	V_c-1 F_r-1 , CE-3
Average surface roughness	1.61			1.80
Cutting temperature	238			202
Grey relation grade	0.6483		0.7971	0.81061

502 Improvement in grey relational grade = $(0.81061 - 0.6483) = 0.16231$ i.e., 25.04 %

503 4. Conclusions

504 In this study, a novel Ag/ZnO hybrid nanofluid was proposed for NFMQL application. Initially,
 505 hybrid Ag coated ZnO nanoparticles were synthesized and characterized. Four nanofluids with
 506 a different volume concentration of these nanoparticles were prepared and characterized for
 507 their thermo-physical properties. Finally, the nanofluid with best characteristics was
 508 implemented for NFMQL application and its performance while machining Inconel 718 was
 509 compared with MQL and dry environments. The following conclusions were drawn from this
 510 study.

- 511 • The Ag coated ZnO hybrid nanoparticles were successfully synthesized by the chemical
 512 precursor process. The hybrid nanofluids comprising of several volume concentrations
 513 ($\Phi = 0.05$ to 0.20%) of Ag/ZnO nanoparticles were characterized for their thermo-

514 physical properties. The nanofluid with 0.20 % concentration of Ag/ZnO particles was
515 found best suitable for NFMQL application.

516 ● The high cutting speed and feed/tooth yielded in a better surface finish, while the lowest
517 cutting temperature was attained at the low cutting speed and feed/tooth values under
518 the NFMQL environment.

519 ● The NFMQL environment also induced a reduced amount of tool wear endorsed by
520 hybrid nanofluid in improving the sliding mechanism, abridged friction at tool-work
521 and chip-tool interfaces. Thus, the NFMQL can be claimed to be a better choice for
522 sustainable production with enhanced product quality.

523 ● The cutting environment was found to significantly contributing by 75.67 % to grey
524 relational grade based on the multi-response characteristics (i.e. for decreasing the
525 cutting temperature whilst enhancing the surface quality). The multi-response
526 optimized machining performance was realised at the cutting speed (level 1): 30 m/min,
527 feed rate (level 1): 0.036 mm/tooth, and NFMQL cutting environment (level 3).

528 In the future work, the effect of different nanofluid concentration, MQL air-pressure and
529 flow rate on material removal rate, surface roughness, cutting temperature and tool wear
530 characteristics (considering the mechanism tool-work interface) are required to be
531 investigated to further validate the performance of proposed nanofluid in this study.

532 **References:**

- 533 1. Unune, D.R. and H.S. Mali, *Parametric modeling and optimization for abrasive*
534 *mixed surface electro discharge diamond grinding of Inconel 718 using response*
535 *surface methodology*. The International Journal of Advanced Manufacturing
536 Technology, 2017. **93**(9-12): p. 3859-3872.

- 537 2. Hegab, H., et al., *Effects of nano-cutting fluids on tool performance and chip*
538 *morphology during machining Inconel 718*. The International Journal of Advanced
539 Manufacturing Technology, 2018. **96**(9-12): p. 3449-3458.
- 540 3. Shukla, A., A. Kotwani, and D.R. Unune, *Performance comparison of dry, flood and*
541 *vegetable oil based minimum quantity lubrication environments during CNC milling*
542 *of Aluminium 6061*. Materials Today: Proceedings, 2019.
- 543 4. Boswell, B., et al., *A review identifying the effectiveness of minimum quantity*
544 *lubrication (MQL) during conventional machining*. The International Journal of
545 Advanced Manufacturing Technology, 2017. **92**(1-4): p. 321-340.
- 546 5. Kumar Mishra, S., S. Ghosh, and S. Aravindan, *Machining performance evaluation of*
547 *Ti6Al4V alloy with laser textured tools under MQL and nano-MQL environments*.
548 Journal of Manufacturing Processes, 2020. **53**: p. 174-189.
- 549 6. Gupta, M.K., et al., *Experimental Investigation and Optimization on MQL-Assisted*
550 *Turning of Inconel-718 Super Alloy*, in *Advanced Manufacturing Technologies*. 2017.
551 p. 237-248.
- 552 7. Singh, G., et al., *Modeling and optimization of tool wear in MQL-assisted milling of*
553 *Inconel 718 superalloy using evolutionary techniques*. The International Journal of
554 Advanced Manufacturing Technology, 2018. **97**(1-4): p. 481-494.
- 555 8. Uzun, İ., K. Aslantas, and F. Bedir, *An experimental investigation of the effect of*
556 *coating material on tool wear in micro milling of Inconel 718 super alloy*. Wear,
557 2013. **300**(1-2): p. 8-19.
- 558 9. Davoodi, B. and A.H. Tazehkandi, *Experimental investigation and optimization of*
559 *cutting parameters in dry and wet machining of aluminum alloy 5083 in order to*
560 *remove cutting fluid*. Journal of Cleaner Production, 2014. **68**: p. 234-242.

- 561 10. Kotwani, A., A. Shukla, and D.R. Unune. *Performance investigation of vegetable oils*
562 *as a cutting fluid in MQL assisted CNC end milling of Al6061*. in *International*
563 *Conference on Precision, Meso, Micro and Nano Engineering (COPEN 2019)*. 2019.
564 IIT Indore.
- 565 11. Gaurav, G., et al., *Assessment of jojoba as a pure and nano-fluid base oil in minimum*
566 *quantity lubrication (MQL) hard-turning of Ti-6Al-4V: A step towards sustainable*
567 *machining*. *Journal of Cleaner Production*, 2020. **272**.
- 568 12. Obikawa, T., Y. Kamata, and J. Shinozuka, *High-speed grooving with applying MQL*.
569 *International Journal of Machine Tools and Manufacture*, 2006. **46**(14): p. 1854-1861.
- 570 13. Barewar, S.D., et al., *Synthesis and thermo-physical properties of water-based novel*
571 *Ag/ZnO hybrid nanofluids*. *Journal of Thermal Analysis and Calorimetry*, 2018.
572 **134**(3): p. 1493-1504.
- 573 14. Yi, S., et al., *Effects of graphene oxide nanofluids on cutting temperature and force in*
574 *machining Ti-6Al-4V*. *The International Journal of Advanced Manufacturing*
575 *Technology*, 2019. **103**(1-4): p. 1481-1495.
- 576 15. Cui, X., et al., *Bio-inspired design of cleaner interrupted turning and its effects on*
577 *specific cutting energy and harmful gas emission*. *Journal of Cleaner Production*,
578 2020. **271**.
- 579 16. Ranga Babu, J.A., K.K. Kumar, and S. Srinivasa Rao, *State-of-art review on hybrid*
580 *nanofluids*. *Renewable and Sustainable Energy Reviews*, 2017. **77**: p. 551-565.
- 581 17. Sarıkaya, M. and A. Güllü, *Multi-response optimization of minimum quantity*
582 *lubrication parameters using Taguchi-based grey relational analysis in turning*
583 *of difficult-to-cut alloy Haynes 25*. *Journal of Cleaner Production*, 2015. **91**: p. 347-
584 357.

- 585 18. Potta, S., *Effect of cryogenic coolant on turning performance: a comparative study*.
586 SN Applied Sciences, 2018. **1**(1).
- 587 19. Jadhav, J. and S. Biswas, *Structural and electrical properties of ZnO:Ag core-shell*
588 *nanoparticles synthesized by a polymer precursor method*. Ceramics International,
589 2016. **42**(15): p. 16598-16610.
- 590 20. Suresh, S., et al., *Effect of Al₂O₃-Cu/water hybrid nanofluid in heat transfer*.
591 Experimental Thermal and Fluid Science, 2012. **38**: p. 54-60.
- 592 21. Singh, G., et al., *Investigations of Machining Characteristics in the Upgraded MQL-*
593 *Assisted Turning of Pure Titanium Alloys Using Evolutionary Algorithms*. Materials,
594 2019. **12**(6).
- 595 22. Khairul, M.A., et al., *Effects of surfactant on stability and thermo-physical properties*
596 *of metal oxide nanofluids*. International Journal of Heat and Mass Transfer, 2016. **98**:
597 p. 778-787.
- 598 23. Chatha, S.S., A. Pal, and T. Singh, *Performance evaluation of aluminium 6063*
599 *drilling under the influence of nanofluid minimum quantity lubrication*. Journal of
600 Cleaner Production, 2016. **137**: p. 537-545.
- 601 24. Bashir, M.A., M. Mia, and N.R. Dhar, *Investigations on Surface Milling of Hardened*
602 *AISI 4140 Steel with Pulse Jet MQL Applicator*. Journal of The Institution of
603 Engineers (India): Series C, 2016. **99**(3): p. 301-314.
- 604 25. Mia, M., et al., *An approach to cleaner production for machining hardened steel*
605 *using different cooling-lubrication conditions*. Journal of Cleaner Production, 2018.
606 **187**: p. 1069-1081.
- 607 26. Yıldırım, Ç.V., et al., *The effect of addition of hBN nanoparticles to nanofluid-MQL*
608 *on tool wear patterns, tool life, roughness and temperature in turning of Ni-based*
609 *Inconel 625*. Tribology International, 2019. **134**: p. 443-456.

- 610 27. Su, Y., et al., *Performance evaluation of nanofluid MQL with vegetable-based oil and*
611 *ester oil as base fluids in turning*. The International Journal of Advanced
612 Manufacturing Technology, 2015. **83**(9-12): p. 2083-2089.
- 613 28. Darshan, C., et al., *Machinability improvement in Inconel-718 by enhanced*
614 *tribological and thermal environment using textured tool*. Journal of Thermal
615 Analysis and Calorimetry, 2019. **138**(1): p. 273-285.
- 616 29. Gatade, V.T., et al., *Experimental investigation of machining parameter under MQL*
617 *milling of SS304*. IOP Conference Series: Materials Science and Engineering, 2016.
618 **149**.
- 619 30. Unune, D.R. and H.S. Mali, *A study of multiobjective parametric optimisation of*
620 *electric discharge diamond cut-off grinding of Inconel 718*. International Journal of
621 Abrasive Technology, 2016. **7**(3).

622